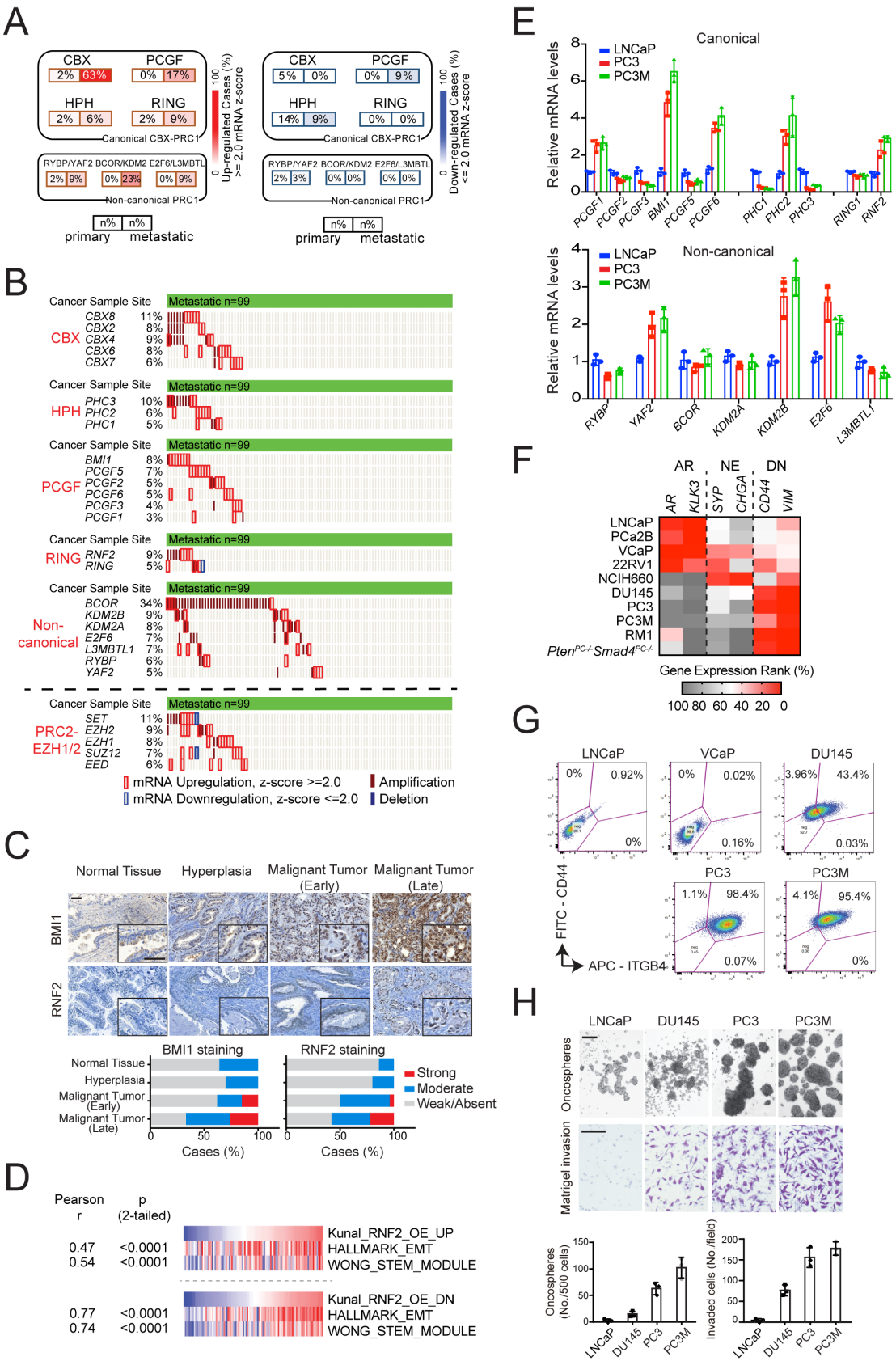

Figure S1, related to Figure 1. Activation of PRC1 in DNPC.

(A) Graphical representation of the mRNA expression profile of PRC1 components in primary vs. metastatic prostate cancers from the Grasso dataset (Grasso et al., 2012). A Z-score of 2.0 was used as a cut-off to determine mRNA up/down-regulation in a given sample. Over and underexpression rates (%) were calculated considering as positive samples with one or more PRC1 subunits up or down-regulated.

(B) Genomic and transcriptional alterations of PRC1 and PRC2 components in the UCSF dataset (n=99) (Quigley et al., 2018). A Z-score of 2.0 was used as a cut-off value to determine mRNA up/down-regulation in a given sample. The Oncoprint was generated using sorted data of mRNA up or down-regulation and gene amplification or deletion information, ordered by aberration rate (%).

(C) Representative immunohistochemical staining of RNF2 (top), BMI1 (middle) and quantification of percentages of cases in each category of staining intensity (bottom) in normal prostate tissues, hyperplasia and malignant tumors (n=128). Scale bar=50 μm. RNF2 or BMI1 staining intensity was classified as Weak/Absent, Moderate, or Strong.

(D) Correlation between the single sample geneset enrichment analysis (ssGSEA) score of RNF2-regulated genesets (Up and Down) and the hallmark epithelial-mesenchymal transition geneset or the androgen response geneset (Liberzon et al., 2015) in the SU2C mCRPC dataset (n=118) (Robinson et al., 2015). Gene expression data was acquired from the cBioportal database. Gene sets of RNF2-upregulated genes (RNF2_OE_UP) and RNF2-downregulated genes (RNF2_OE_DN) were retrieved from a previous study (Rai et al., 2015). ssGSEA Projection module (version 9.0.10, genepatter.org) was used to calculate the enrichment score of individual samples.

(E) Relative mRNA levels of the genes encoding canonical and non-canonical PRC1 components in LNCaP, PC3 and PC3M cells. The error bars represent the mean±SD of triplicate experiments.

(F) Heatmap of gene expression from the indicated prostate cancer cell lines classified based on their AR, NE, and DN gene expression rank. Genes were ordered by their reads per kilobase million (RPKM) values in each sample. The heatmap was generated by using the percentage ranking of selected marker genes (for AR: *AR* and *KLK3*; for NE, *SYP* and *CHGA*; for DN: *CD44* and *VIM*). There was no detectable expression of *KLK3* orthologues or *SYP* transcript in the RM1 and $Pten^{PC-/-}Smad4^{PC-/-}$ cells.

(G) Cell surface expression of CD44 and ITGB4 in the indicated prostate cancer cell lines. LNCaP, VCaP, DU145, PC3 and PC3M cells were stained with anti-CD44-FITC and anti-ITGB4-APC antibodies and subjected to Flow Cytometry analysis.

(H) Representative images of tumor sphere formation (top), invasion through Matrigel (middle) and graph quantifications (bottom) of selected human prostate cancer cells. The indicated cells were plated in triplicate in 24 well ultra-low attachment plates or Matrigel coated chambers at a seeding density of 1,000 cells/well (sphere assay) or 2 x 10^4 cells/well (Matrigel invasion assay). Numbers of spheres were counted after 7 days; invasive cells were counted 16 hours after plating. Scale bar=200 μm in sphere images, bar=100 μm in Matrigel invasion images. The error bars represent the mean±SD of triplicate experiments.

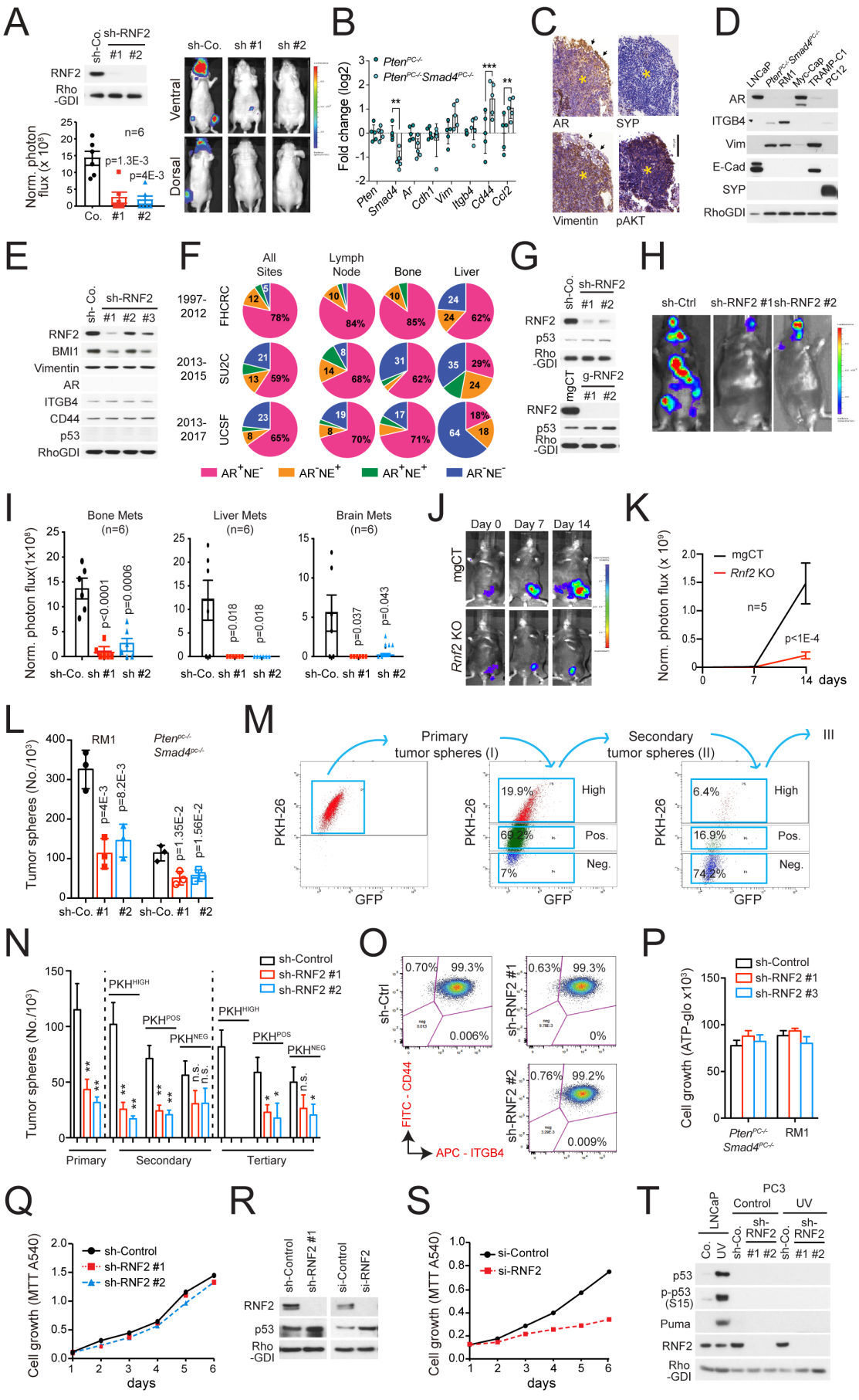
A
sh-Co.
sh-RNF2
#1 #2
RNF2
Rho -GDI
Norm. photon flux (x 10⁶)
n=6
p=1.3E-3
p=4E-3
Co. #1 #2
sh-Co. sh #1 sh #2
Ventral
Dorsal
B
Ptenpc-/-
Ptenpc-/-Smad4pc-/-
Fold change (log2)
Pten Smad4 Ar Cdh1 Vim Itgb4 Cd44 Ccl2
C
AR
SYP
Vimentin
pAKT
D
LNCaP
Ptenpc-/-Smad4pc-/-
RM1
Myc-CaP
TRAMP-C1
PC12
AR
ITGB4
Vim
E-Cad
SYP
RhoGDI
E
sh-Co.
sh-RNF2
#1 #2 #3
RNF2
BMI1
Vimentin
AR
ITGB4
CD44
p53
RhoGDI
F
All Sites
Lymph Node
Bone
Liver
1997-2012 FHCRC
2013-2015 SU2C
2013-2017 UCSF
AR+NE-
AR-NE+
AR+NE+
AR-NE-
G
sh-Co.
sh-RNF2
#1 #2
RNF2
p53
Rho -GDI
mgCT
g-RNF2
#1 #2
RNF2
p53
Rho -GDI
H
sh-Ctrl
sh-RNF2 #1
sh-RNF2 #2
I
Bone Mets (n=6)
Liver Mets (n=6)
Brain Mets (n=6)
Norm. photon flux(1x10⁶)
p<0.0001
p=0.0006
p=0.018
p=0.018
p=0.037
p=0.043
sh-Co. sh #1 sh #2
J
Day 0
Day 7
Day 14
mgCT
Rnf2 KO
K
Norm. photon flux (x 10⁹)
mgCT
Rnf2 KO
n=5
p<1E-4
0 7 14 days
L
RM1
Ptenpc-/-Smad4pc-/-
Tumor spheres (No./10³)
p=4E-3
p=8.2E-3
p=1.35E-2
p=1.56E-2
sh-Co. #1 #2 sh-Co. #1 #2
M
Primary tumor spheres (I)
Secondary tumor spheres (II)
III
PKH-26
GFP
19.9%
High
Pos.
Neg.
7%
6.4%
16.9%
74.2%
N
sh-Control
sh-RNF2 #1
sh-RNF2 #2
Tumor spheres (No./10³)
PKHHIGH
PKHPOS
PKHNEG
n.s.
Primary
Secondary
Tertiary
O
sh-Ctrl
sh-RNF2 #1
sh-RNF2 #2
0.70%
99.3%
0.006%
0.63%
99.3%
0%
0.76%
99.2%
0.009%
FITC - CD44
APC - ITGB4
P
sh-Control
sh-RNF2 #1
sh-RNF2 #3
Cell growth (ATP-glo x10³)
Ptenpc-/-Smad4pc-/-
RM1
Q
sh-Control
sh-RNF2 #1
sh-RNF2 #2
Cell growth (MTT A540)
days
R
sh-Control
sh-RNF2 #1
si-Control
si-RNF2
RNF2
p53
Rho -GDI
S
si-Control
si-RNF2
Cell growth (MTT A540)
days
T
LNCaP
PC3
Control
UV
Co.
UV
sh-Co.
sh-RNF2 #1 #2
sh-Co.
sh-RNF2 #1 #2
p53
p-p53 (S15)
Puma
RNF2
Rho -GDI

Figure S2, related to Figure 2. PRC1 is required for tumor initiation and metastasis.

(A) RNF2 knockdown efficiency (left top), quantification of luciferase counts (left bottom) and representative images (right) of male nude mice at 4 weeks after injected intracardially (i.c.) with 2.5 x 10^5 luciferase labeled control and RNF2-silenced PC3M cells. Bars, mean±SEM.

(B) The expression levels of the indicated genes in *Pten*$^{PC-/-}$*Smad4*$^{PC-/-}$ tumors is shown as fold change over that in *Pten*$^{PC-/-}$ tumors, bars, mean±SD. RNAseq data were from the anterior prostates of 15 weeks-old mice (GSE25140; Wang at al., 2015). Two-way ANOVA, corrected for multiple comparisons by Sidak's method, **p <0.01, *** p<0.001.

(C) Immunohistochemical staining of AR, NE marker synaptophysin, mesenchymal marker vimentin, and tumor cell marker pAKT in *Pten*$^{PC-/-}$*Smad4*$^{PC-/-}$ tumors. Yellow asterisks indicate area of DNPC (AR-negative, vimentin-positive, synaptophysin-negative) adjacent to AR-positive cancer cells (white-dotted area, black arrows). Prostate tumor tissues were collected from 9 months-old mice and subjected to immunohistochemical staining using the indicated antibodies, bar=100 μm.

(D) Immunoblotting of the indicated AR signaling, hybrid E/M, and NE markers in mouse prostate cancer cell lines.

(E) Lysates from control and RNF2-silenced *Pten*$^{PC-/-}$*Smad4*$^{PC-/-}$ cells were subjected to immunoblotting with the indicated antibodies.

(F) Pie charts showing the frequency of AR-active prostate cancers (PCa) (AR^+NE^-), neuroendocrine PCa (AR^-NE^+), double-negative PCa (AR^-NE^-), and double-positive PCa (AR^+NE^+) in three metastatic CRPC datasets. Samples were categorized according to site of metastasis (lymph node metastases and distant bone or liver metastases). Years indicate sample acquisition period. FHCRC (Kumar et al., 2016) and SU2C transcriptome/clinical data were acquired via cBioPortal. UCSF (Quigley et al., 2018) data were generously provided by the authors (Reference: FHCRC – PMID 26928463; SU2C – PMID 26000489; UCSF – PMID 30033370).

(G) Verification of *Rnf2* knockdown (top) or knockout (bottom) efficiency in RM1 cells by immunoblotting.

(H and I) Representative images (H) and quantification of luciferase counts (I) of male C57B6 mice at 3 weeks after injected i.c. with 3 x 10^4 control and RNF2-silenced RM1 cells. Bars, mean±SD.

(J and K) Representative images (J) and quantification of luciferase counts (K) of male C57B6 mice with intra-femoral artery injection of 1x10^4 control or *Rnf2* knockout RM1 cells. Bars, mean±SD.

(L) Quantification of control and RNF2-silenced RM1 or *Pten*$^{PC-/-}$*Smad4*$^{PC-/-}$ cells subjected to sphere assay at day 5. Cells were plated at a seeding density of 1,000 cells/well. Bars, mean±SD of triplicate experiments.

(M) FACS analysis for PKH-26 and GFP staining during serial tumor sphere assay of GFP-tagged PC3 cells. Cells were stained with PKH-26 and subjected to tumor sphere assay. Primary tumor spheres were dissociated and their constituent cells were sorted according to PKH-26 staining intensity (PKH^{HIGH}, PKH^{POS} and PKH^{NEG}) (center) and subjected to secondary tumor sphere assay. Finally, the PKH^{HIGH} tumor cells from secondary tumor spheres were subjected to the same assay to derive tertiary tumor spheres.

(N) Quantification of control and RNF2-silenced PC3 cells stained with PKH-26 and subjected to serial tumor sphere assay as described above. The graphs show the number of tumor spheres formed at each passage by PKH^{HIGH}, PKH^{POS} and PKH^{NEG} tumor cells. Bars, mean±SD of triplicate experiments, * $p < 0.05$; ** $p < 0.01$; n.s. not significant.

(O) Flow Cytometry analysis of PC3 cells stably expressing the indicated constructs.

(P) Cell growth analysis of control and RNF2-silenced *Pten*$^{PC-/-}$*Smad4*$^{PC-/-}$ or RM1 cells plated in 96-well plates at a seeding density of 2,000 cells/well. Cell growth was measured by the ATP-Glo assay at 72 hours after plating, bars, mean±SD.

(Q) Cell growth analysis of control and RNF2-silenced PC3 cells plated in 96 well plates at a seeding density of 2,000 cells/well. Cell growth rates were measured by MTT assay at the indicated times.

(R) Immunoblotting of LNCaP cells transiently transfected with the indicated constructs.

(S) Cell growth analysis of control and RNF2-silenced LNCaP cells plated in 96 well plates at a seeding density of 2,000 cells/well. Cell growth rates were measured by MTT assay at the indicated times.

(T) LNCaP or PC3 cells expressing the indicated constructs were subjected to UV treatment. Lysates were collected and subjected to immunoblotting.

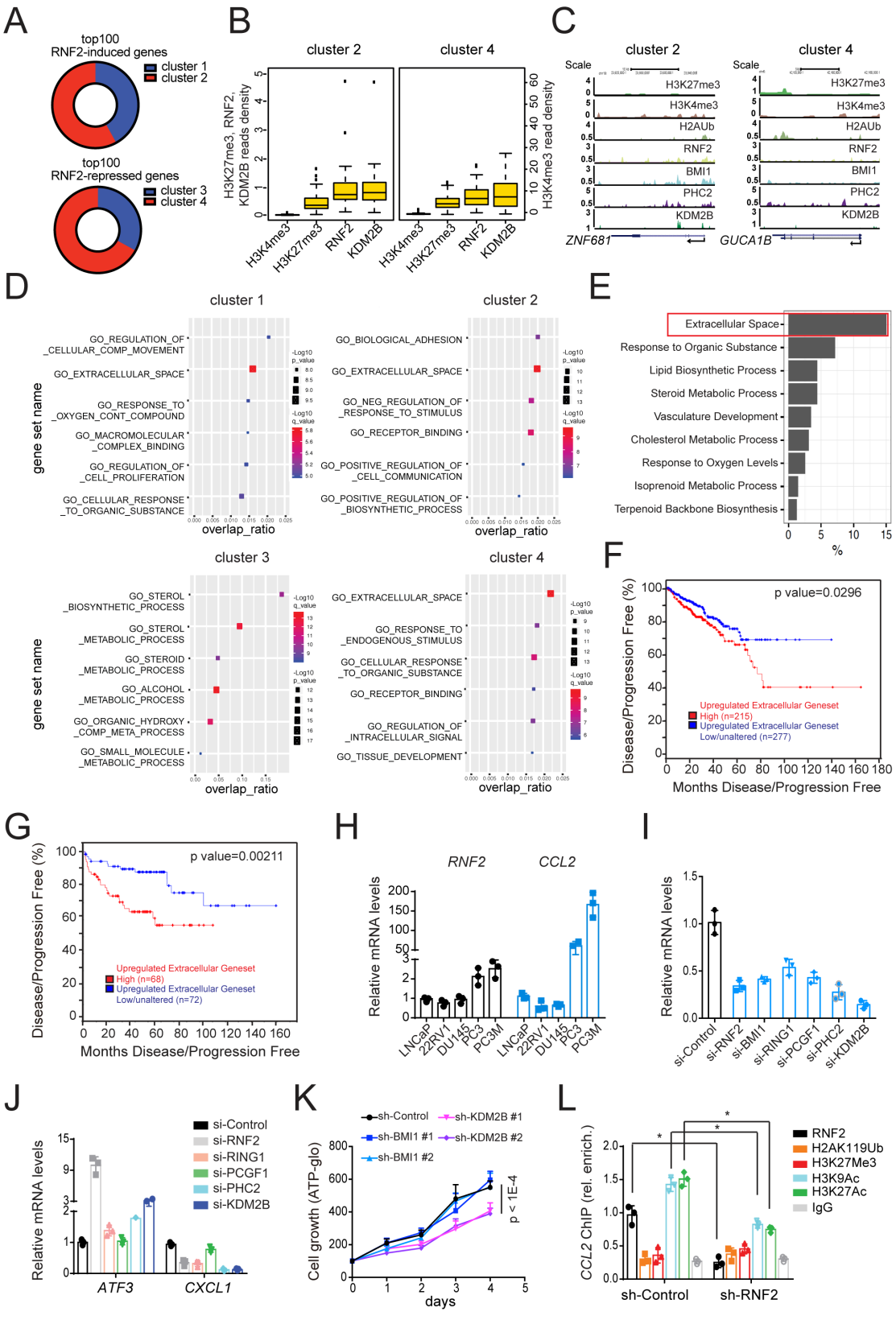
A
top100
RNF2-induced genes
cluster 1
cluster 2
top100
RNF2-repressed genes
cluster 3
cluster 4
B
cluster 2
cluster 4
H3K27me3, RNF2, KDM2B reads density
H3K4me3 read density
H3K4me3
H3K27me3
RNF2
KDM2B
C
cluster 2
cluster 4
Scale
H3K27me3
H3K4me3
H2AUb
RNF2
BMI1
PHC2
KDM2B
ZNF681
GUCA1B
D
cluster 1
cluster 2
cluster 3
cluster 4
gene set name
GO_REGULATION_OF_CELLULAR_COMP_MOVEMENT
GO_EXTRACELLULAR_SPACE
GO_RESPONSE_TO_OXYGEN_CONT_COMPOUND
GO_MACROMOLECULAR_COMPLEX_BINDING
GO_REGULATION_OF_CELL_PROLIFERATION
GO_CELLULAR_RESPONSE_TO_ORGANIC_SUBSTANCE
GO_BIOLOGICAL_ADHESION
GO_NEG_REGULATION_OF_RESPONSE_TO_STIMULUS
GO_RECEPTOR_BINDING
GO_POSITIVE_REGULATION_OF_CELL_COMMUNICATION
GO_POSITIVE_REGULATION_OF_BIOSYNTHETIC_PROCESS
GO_STEROL_BIOSYNTHETIC_PROCESS
GO_STEROL_METABOLIC_PROCESS
GO_STEROID_METABOLIC_PROCESS
GO_ALCOHOL_METABOLIC_PROCESS
GO_ORGANIC_HYDROXY_COMP_META_PROCESS
GO_SMALL_MOLECULE_METABOLIC_PROCESS
GO_RESPONSE_TO_ENDOGENOUS_STIMULUS
GO_REGULATION_OF_INTRACELLULAR_SIGNAL
GO_TISSUE_DEVELOPMENT
overlap_ratio
E
Extracellular Space
Response to Organic Substance
Lipid Biosynthetic Process
Steroid Metabolic Process
Vasculature Development
Cholesterol Metabolic Process
Response to Oxygen Levels
Isoprenoid Metabolic Process
Terpenoid Backbone Biosynthesis
%
F
p value=0.0296
Disease/Progression Free (%)
Upregulated Extracellular Geneset
High (n=215)
Upregulated Extracellular Geneset
Low/unaltered (n=277)
Months Disease/Progression Free
G
p value=0.00211
Disease/Progression Free (%)
Upregulated Extracellular Geneset
High (n=68)
Upregulated Extracellular Geneset
Low/unaltered (n=72)
Months Disease/Progression Free
H
RNF2
CCL2
Relative mRNA levels
LNCaP
22RV1
DU145
PC3
PC3M
I
Relative mRNA levels
si-Control
si-RNF2
si-BMI1
si-RING1
si-PCGF1
si-PHC2
si-KDM2B
J
Relative mRNA levels
si-Control
si-RNF2
si-RING1
si-PCGF1
si-PHC2
si-KDM2B
ATF3
CXCL1
K
sh-Control
sh-KDM2B #1
sh-BMI1 #1
sh-KDM2B #2
sh-BMI1 #2
Cell growth (ATP-glo)
p < 1E-4
days
L
CCL2 ChIP (rel. enrich.)
RNF2
H2AK119Ub
H3K27Me3
H3K9Ac
H3K27Ac
IgG
sh-Control
sh-RNF2

Figure S3, related to Figure 3. PRC1 promotes the expression of *CCL2* and other pro-metastatic genes.

(A) Pie charts showing the proportion of cluster 1 and 2 genes amongst the top 100 genes induced by RNF2 (top) and the proportion of cluster 3 and 4 genes amongst the top 100 genes repressed by RNF2 (bottom).

(B) Boxplot of the average reads densities for H3K27me3, H3K27me3, RNF2 and KDM2B at the core promoter regions of genes in clusters 2 and 4. Core promoter regions are defined as ±500 bp around TSS sites. Reads densities are calculated by average reads densities across core promoter regions. Standard boxplot was applied to diplay the distribution of the values of average reads densities based on a 5-number summary ("minimum", first quartile (Q1), median, third quartile (Q3), and "maximum"). The median value is depicted as a line splitting the box in half. The middle "box" represents the middle 50% of scores for the group. The upper and lower whickers represent scores outside the middle 50%. Outlier as points extending beyond the whiskers.

(C) UCSC Genome Browser view of the H3K4me3, H3K27me3, H2AUb, RNF2, BMI1, PHC2 and KDM2B peaks for the indicated representative genes in clusters 2 and 4.

(D) Gene ontology (GO) analysis of the genes in each cluster. The graphs show the top 6 gene signatures in each cluster. The X axis (overlap-ratio) represents the ratio of the number of overlapping genes to the number of genes in each signature.

(E) GO enrichment and KEGG pathway analysis of differentially expressed genes according to biological processes. Top 9 GO terms enriched among differentially expressed genes upon RNF2 silencing. The percentage of differentially expressed genes in a pathway was used for the analysis.

(F and G) Kaplan–Meier analysis of the TCGA (n=498) (The Cancer Genome Atlas Research, 2015) (F) and Taylor (n=150) (Taylor et al., 2010) (G) prostate cancer datasets showing the disease-free survival of patients separated in 2 cohorts based on the expression of RNF2-activated genes from the Extracellular Space category.

(H) Quantitative RT-PCR showing the levels of expression of *RNF2* and *CCL2* in the indicated prostate cancer cell lines. Bars, mean±SD of triplicate experiments.

(I) Quantitative RT-PCR showing the levels of expression of *CCL2* in PC3 cells transfected with the indicated siRNAs for 48 hours. Bars, mean±SD of triplicate experiments.

(J) Quantitative RT-PCR showing the levels of expression of *ATF3* and *CXCL1* in PC3 cells transfected with the indicated siRNAs for 48 hours. Bars, mean±SD of triplicate experiments.

(K) Cell growth analysis of PC3 cells stably expressing the indicated constructs plated in 96 well plates at a seeding density of 2,000 cells/well. Cell growth was measured by ATP-Glo assay at the indicated times. Bars, mean±SD.

(L) Relative occupancy of RNF2, H2AK119Ub, H3K27me3, H3K9Ac, H3K27Ac and IgG control on the *CCL2* promoter from ChIP-qPCR in control or RNF2-silenced PC3M cells; bars, mean±SD of triplicate experiments. * $p < 0.05$.

Table S2, related to Figure 3. List of Extracellular Space pathway genes regulated by RNF2.

Genes activated by RNF2 (upregulated geneset)	Genes repressed by RNF2 (downregulated geneset)
ACPL2	ADM2
ANGPT1	CPZ
ANGPTL2	CTSS
ANGPTL4	CYR61
APLN	EFEMP2
C11orf45	FBN1
C3	FGF1
C6orf58	FGFBP1
CCL2	GDF15
CCL28	GDF5
CHI3L2	GNRH1
CILP2	HAPLN2
CRLF1	IL18
CSF3	IL1A
CXCL1	IL32
DHRS13	IL7R
F2RL2	LDLR
HHIPL2	LEPR
IGF2	LIF
IL4R	LIPG
ISM1	MICA
LCN2	MMRN2
LFNG	MST1
LOX	MUC13
LRG1	NTS
NOG	PAPPA2
PDZD2	PLAU
PI3	PNLIPRP3
PLA2G7	RELN
SAA1	SPINK1
SEMA3B	SPINK13
SERPIND1	STRCP1

SFRP4	TCN1
SLPI	TENM1
STC1	THBS3
SULF2	THBS4
TNFAIP2	TNXB
UMODL1	UTS2
UTS2B	
VASH1	
VLDLR	
VNN3	
WISP1	
ZP1	

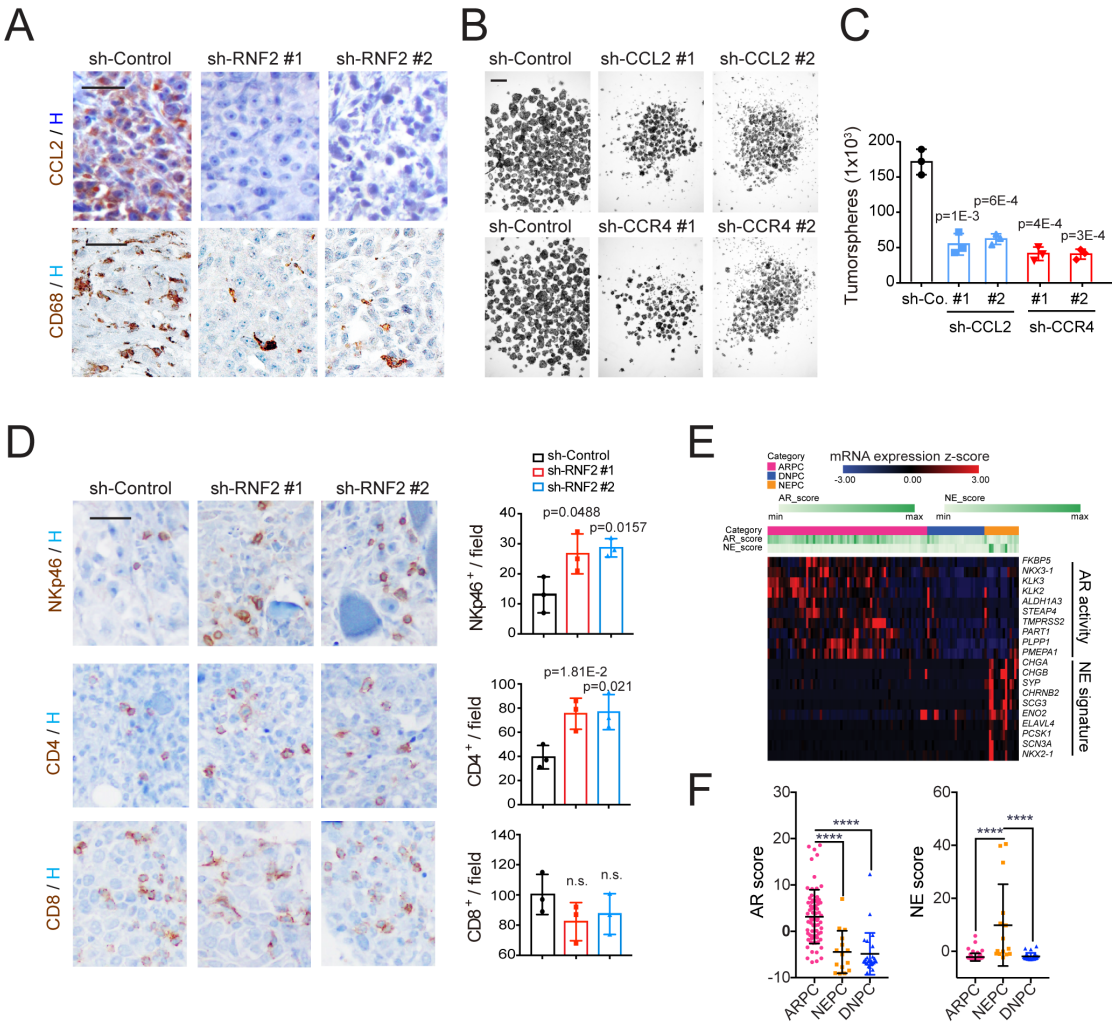
A
sh-Control
sh-RNF2 #1
sh-RNF2 #2
CCL2 / H
CD68 / H
B
sh-Control
sh-CCL2 #1
sh-CCL2 #2
sh-Control
sh-CCR4 #1
sh-CCR4 #2
C
Tumorspheres (1x10³)
200
150
100
50
0
p=1E-3
p=6E-4
p=4E-4
p=3E-4
sh-Co.
#1
#2
#1
#2
sh-CCL2
sh-CCR4
D
sh-Control
sh-RNF2 #1
sh-RNF2 #2
NKp46 / H
CD4 / H
CD8 / H
sh-Control
sh-RNF2 #1
sh-RNF2 #2
NKp46⁺ / field
p=0.0488
p=0.0157
CD4⁺ / field
p=1.81E-2
p=0.021
CD8⁺ / field
n.s.
n.s.
E
Category
ARPC
DNPC
NEPC
mRNA expression z-score
-3.00
0.00
3.00
AR_score
NE_score
min
max
min
max
Category
AR_score
NE_score
FKBP5
NKX3-1
KLK3
KLK2
ALDH1A3
STEAP4
TMPRSS2
PART1
PLPP1
PMEPA1
CHGA
CHGB
SYP
CHRNB2
SCG3
ENO2
ELAVL4
PCSK1
SCN3A
NKX2-1
AR activity
NE signature
F
AR score
NE score
****
****
****
****
ARPC
NEPC
DNPC
ARPC
NEPC
DNPC

Figure S4, related to Figure 4. Targeting PRC1-CCL2 signaling impairs bone metastasis.

(A) Representative images of immunohistochemical staining for CCL2 or CD68 of end point subcutaneous tumors from PC3 cells injected nude mice; bar=50 μm.

(B and C) Representative images (B) and quantification (C) of control and CCL2/CCR4-silenced PC3 cells subjected to sphere assay at day 7. Scale bar=200 μm. Error bars, mean±SD of triplicate experiments.

(D) Representative images (left, bar=50 μm) and quantification of positive NK or T cells (right, bars, mean±SD of triplicate experiments) in bone tissues from mice injected i.c. with RM1 cells collected at the end point of experiment.

(E) Classification of the SU2C M-CRPC dataset by molecular subtype (ARPC, NEPC, DNPC). Subtype classification and AR activity score and NE signature score were calculated as previously described (Bluemn et al., 2017). Supervised hierarchical clustering of the SU2C M-CRPC dataset by AR and NE scoring genesets. ARPC (n=70, 64%), DNPC (n=25, 23%), NEPC (n=15, 14%). DPPC (n=8) was not included in the analysis. AR/DN/NE molecular subtype and the AR/NE score were depicted on top of the heatmap. Metric: Euclidean distance; linkage method: average.

(F) The classified groups from (E) were compared by using one-way ANOVA and multiple comparisons test by Benjamni, Krieger and Yekutieli two-stage step-up method. Bars, mean±SD, **** $p < 0.0001$.

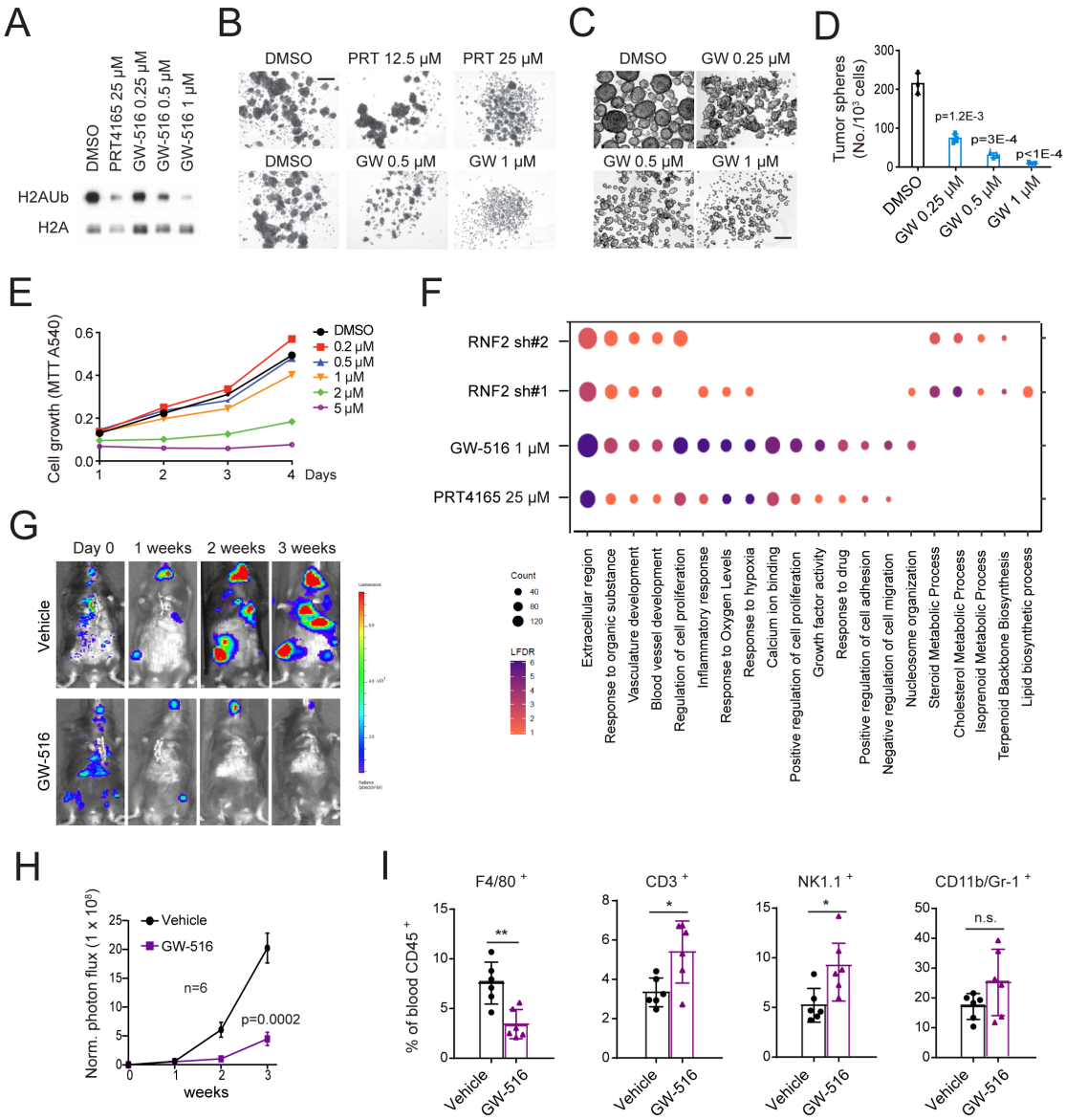
A
DMSO
PRT4165 25 μM
GW-516 0.25 μM
GW-516 0.5 μM
GW-516 1 μM
H2AUb
H2A
B
DMSO
PRT 12.5 μM
PRT 25 μM
DMSO
GW 0.5 μM
GW 1 μM
C
DMSO
GW 0.25 μM
GW 0.5 μM
GW 1 μM
D
Tumor spheres (No./10³ cells)
p=1.2E-3
p=3E-4
p<1E-4
DMSO
GW 0.25 μM
GW 0.5 μM
GW 1 μM
E
Cell growth (MTT A540)
DMSO
0.2 μM
0.5 μM
1 μM
2 μM
5 μM
Days
F
RNF2 sh#2
RNF2 sh#1
GW-516 1 μM
PRT4165 25 μM
Count
LFDR
Extracellular region
Response to organic substance
Vasculature development
Blood vessel development
Regulation of cell proliferation
Inflammatory response
Response to Oxygen Levels
Response to hypoxia
Calcium ion binding
Positive regulation of cell proliferation
Growth factor activity
Response to drug
Positive regulation of cell adhesion
Negative regulation of cell migration
Nucleosome organization
Steroid Metabolic Process
Cholesterol Metabolic Process
Isoprenoid Metabolic Process
Terpenoid Backbone Biosynthesis
Lipid biosynthetic process
G
Day 0
1 weeks
2 weeks
3 weeks
Vehicle
GW-516
H
Norm. photon flux (1 x 10⁶)
Vehicle
GW-516
n=6
p=0.0002
weeks
I
F4/80 +
CD3 +
NK1.1 +
CD11b/Gr-1 +
% of blood CD45 +
**
*
*
n.s.
Vehicle
GW-516

Figure S5, related to Figure 5. Development of a catalytic inhibitor of PRC1.

(A) Immunoblotting of PC3 cells treated with 25 μM PRT4165 and the indicated doses of GW-516 for 24 hours. Acid extracts of nuclei were prepared and immunoblotted using H2A and H2AK119Ub antibodies.

(B) Representative images of PC3 tumor spheres treated with PRT4165 or GW-516 at the indicated doses, bar=200 μm.

(C and D) Representative images (C) and quantifications of tumor spheres (D) of RM1 cells treated with different doses of GW-516 as indicated. Scale bar=200 μm. Error bars, mean±SD.

(E) Cell growth analysis of PC3 cells treated with GW-516 at the indicated doses. Cells were plated at a density of 2,000 cells/well. Cell growth rates were measured by MTT assay at the indicated times.

(F) GO enrichment and KEGG pathway analysis of the differentially expressed genes in RNF2-silenced and GW-516 or PRT4165 treated PC3 cells. The size of each dot is proportional to the total number of differentially expressed genes in each pathway. Color scale represents LFDR (-Log10 FDR).

(G and H) Representative images (G) and cumulative luciferase counts (H) of mice injected i.c. with 3 x 10^4 RM1 cells and subsequently treated with vehicle (DMSO) or GW-516 (25 mg/kg). Treatment was started at day 7 post-injection. Mice were dosed twice per week. Bars, mean±SEM.

(I) FACS analysis of immune cell subsets in the blood of end point mice from (G). Blood cells were collected at day 21 post-injection and stained with indicated antibodies,; bars, mean±SD. * $p < 0.05$, ** $p < 0.01$.

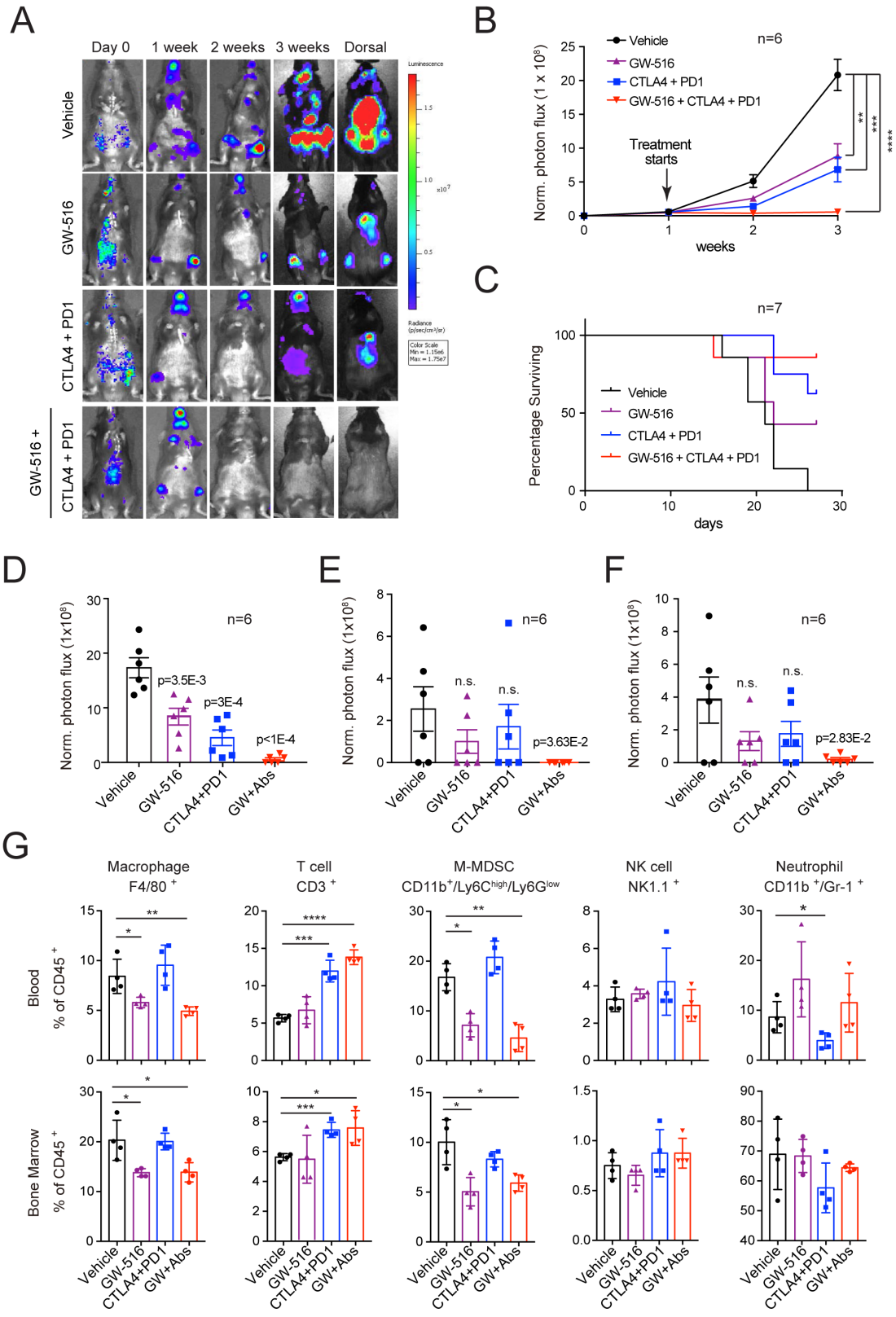
A
Day 0
1 week
2 weeks
3 weeks
Dorsal
Vehicle
GW-516
CTLA4 + PD1
GW-516 +
CTLA4 + PD1
B
n=6
Vehicle
GW-516
CTLA4 + PD1
GW-516 + CTLA4 + PD1
Norm. photon flux (1 x 10⁸)
Treatment starts
weeks
C
n=7
Percentage Surviving
days
D
n=6
Norm. photon flux (1x10⁸)
p=3.5E-3
p=3E-4
p<1E-4
E
n=6
n.s.
n.s.
p=3.63E-2
F
n=6
n.s.
n.s.
p=2.83E-2
Vehicle
GW-516
CTLA4+PD1
GW+Abs
G
Macrophage
F4/80 +
T cell
CD3 +
M-MDSC
CD11b+/Ly6Chigh/Ly6Glow
NK cell
NK1.1 +
Neutrophil
CD11b +/Gr-1 +
Blood
% of CD45 +
Bone Marrow
% of CD45 +

Figure S6, related to Figure 6. Pharmacological inhibition of PRC1 cooperates with immunotherapy to suppress metastasis.

(A-C) Representative images (A), cumulative luciferase counts (B) and survival analysis (C) of male C57B6 mice injected i.c. with 3 x 10^4 RM1 cells and subsequently treated with vehicle (control IgG), PD-1 and CTLA-4 antibodies (anti-mouse PD-1: 200 µg/mouse; anti-mouse CTLA-4: 250 µg/mouse), GW-516 (10 mg/kg), and GW-516 plus PD-1 and CTLA-4 antibodies. Treatment was started at day 7 post-injection. Mice were dosed twice per week. Bars, mean±SEM. ** $p < 0.01$; *** $p < 0.005$; **** $p < 0.0001$.

(D-F) Quantification of luciferase counts in the bone (D), liver (E) and brain (F) of end point mice from (A); bars, mean±SEM.

(G) FACS analysis of immune cell subsets in the blood and bone marrow of end point mice from (A). Bars, mean±SD. * $p < 0.05$; ** $p < 0.01$; *** $p < 0.005$; **** $p < 0.0001$.

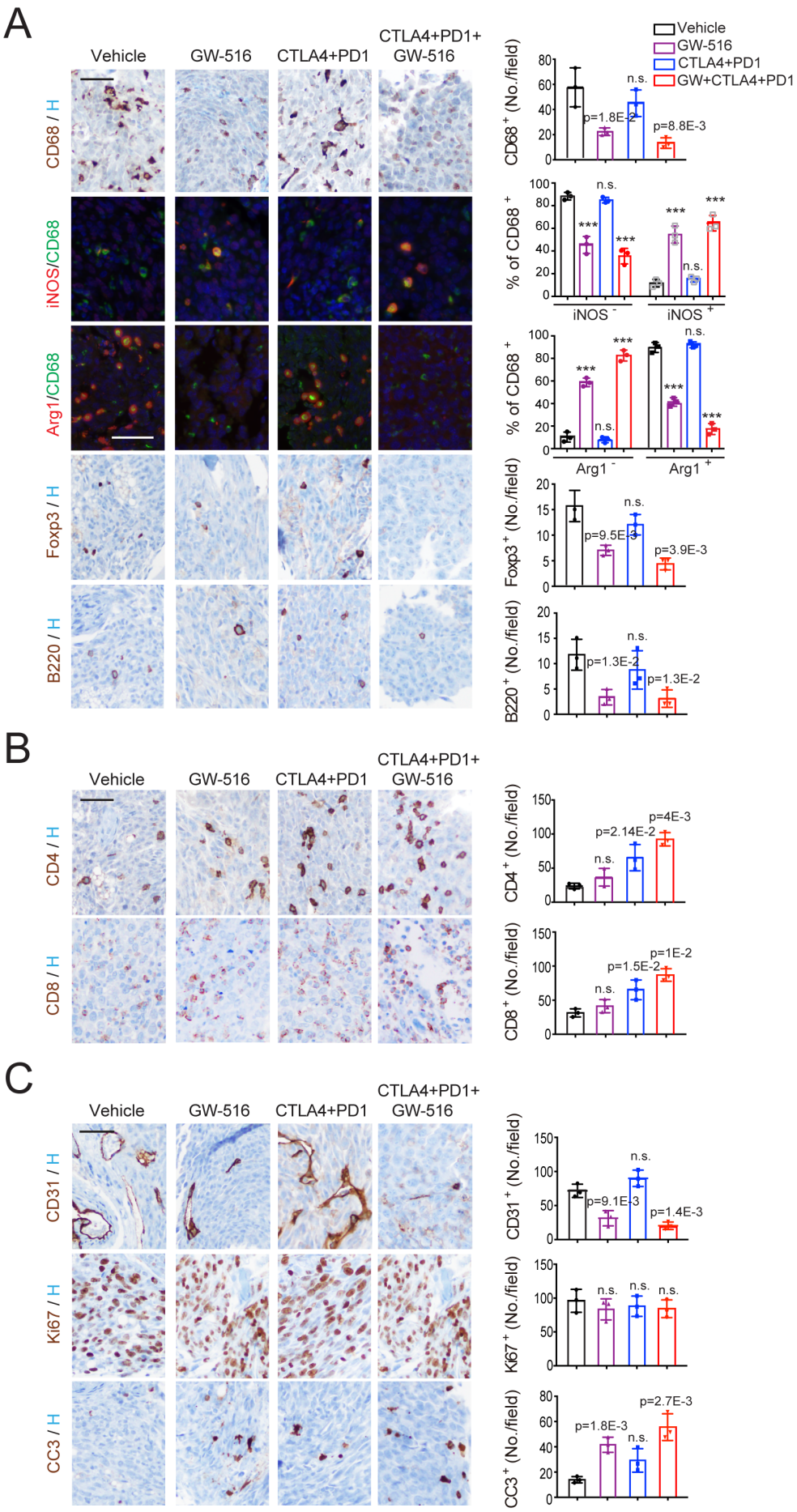
A
Vehicle
GW-516
CTLA4+PD1
CTLA4+PD1+ GW-516
CD68 / H
iNOS/CD68
Arg1/CD68
Foxp3 / H
B220 / H
Vehicle
GW-516
CTLA4+PD1
GW+CTLA4+PD1
CD68+ (No./field)
p=1.8E-2
n.s.
p=8.8E-3
% of CD68+
iNOS-
iNOS+
Arg1-
Arg1+
Foxp3+ (No./field)
p=9.5E-3
p=3.9E-3
B220+ (No./field)
p=1.3E-2
p=1.3E-2
B
CD4 / H
CD8 / H
CD4+ (No./field)
p=2.14E-2
p=4E-3
CD8+ (No./field)
p=1.5E-2
p=1E-2
C
CD31 / H
Ki67 / H
CC3 / H
CD31+ (No./field)
p=9.1E-3
p=1.4E-3
Ki67+ (No./field)
CC3+ (No./field)
p=1.8E-3
p=2.7E-3

Figure S7, related to Figure 7. Pharmacological inhibition of PRC1 reverses immune suppression and cooperates with immunotherapy to suppress metastasis.

(A-C) Representative staining images (left, bar=50 μm) and quantifications of positive cell (right, bars, mean±SD, *** $p < 0.005$) for immune-suppressive cells (A), T cells (B), and endothelial cells and proliferating/apoptotic tumor cells (C) in bone tissues from mice injected i.c. with RM1 cells collected after 1 week of treatment and subjected to IHC or IF staining.

Click here to access/download

Supplemental Videos and Spreadsheets

Table S1.xlsx